Theor Chem Acc (2014) 133:1436
DOI 10.1007/s00214-013-1436-7

REGULAR ARTICLE

Accurate first principles calculations on chlorine fluoride ClF and its ions $ClF^{\pm}$

Athanassios A. Vassilakis · Apostolos Kalemos · Aristides Mavridis

Received: 12 September 2013 / Accepted: 5 December 2013

Abstract The present work focuses on the first (lightest) of the six diatomic interhalogens, namely ClF and its ions ClF^+ and ClF^-, in an effort to better understand these interesting species. Toward this end, we have performed highly correlated all electron ab initio calculations of multireference (MRCI) and single-reference coupled-cluster calculations, employing quintuple and sextuple correlation consistent basis sets. Within the $\Lambda - S$ ansatz, we have examined all 12 states of ClF correlating adiabatically with the first energy channel, all 23 states of ClF^+ correlating with the first three channels, and three states out of four of ClF^- correlating with the first two channels $Cl^- + F$ and $Cl + F^-$. Full potential energy curves at the MRCI/quintuple zeta level have been constructed for 12, 21, and 3 states of ClF, ClF^+, and ClF^-, respectively. After correcting for core–subvalence and scalar relativistic effects, albeit small as expected, and spin–orbit interactions, most of our results are in excellent agreement with available experimental data. Some lingering questions have been definitely settled. Our final recommended binding energies (D_0 in kcal/mol) and equilibrium bond distances (r_e in Å) for ClF ($X\ ^1\Sigma^+$), ClF^+ ($X\ ^2\Pi$), and ClF^- ($X\ ^2\Sigma^+$) are [60.35, 1.6284], [67.40, 1.5357], and [29.80, 2.151], respectively. The adiabatic electron affinity of ClF, ClF ($X\ ^1\Sigma^+$) + $e^- \rightarrow ClF^-$ ($X\ ^2\Sigma^+$), is $EA_{ad} = 2.25 \pm 0.01$ eV about 0.6 eV smaller than the suggested experimental value which is certainly wrong.

Keywords Interhalogen · ClF · Ab initio

1 Introduction

One of the most interesting series of atomic elements are the four stable halogens (X), namely ^{19}F ($Z = 9$), $^{35,37}Cl$ (17), $^{79,81}Br$ (35), and ^{127}I (53) [1]. All possible combinations between the four halogens result to four homonuclear dihalides (X_2) and six unique diatomic interhalogens (XX′), viz. ClF, BrF, IF, BrCl, ICl, and IBr, all of which are known and relatively stable, the most robust being the ClF [2]. The latter is a colorless gas at room temperature with a melting point of −155.6 °C [2] and a dissociation energy (D_0^0) of ~60 kcal/mol [3]. For some physical properties of the XX′ compounds, see Table 17.12 of Ref. [2].

The present ab initio work focuses on ClF and its ions ClF^+ and ClF^-. We have investigated all 12 $^{2S+1}\Lambda$ molecular states of the neutral species emanating from the ground-state fragments Cl(^{2}P) and F(^{2}P), all 23 (=12 + 9+2) states of ClF^+ related to the first three adiabatic channels of Cl^+(^{3}P, ^{1}D, ^{1}S) + F(^{2}P), and three states of ClF^-, employing variational multireference (MRCI) and single-reference coupled cluster methods combined with large correlation consistent basis sets. In what follows we give a rather complete account of the previous experimental and theoretical work on ClF and $ClF^{\pm}$ related to the present work.

To the best of our knowledge, the first experimental work on ClF was published by Wahrhaftig [4] in 1942 who

Dedicated to Professor Thom Dunning and published as part of the special collection of articles celebrating his career upon his retirement.

A. A. Vassilakis · A. Kalemos · A. Mavridis (✉)
Laboratory of Physical Chemistry, Department of Chemistry, National and Kapodistrian University of Athens, Panepistimiopolis, Athens 157 71, Greece
e-mail: mavridis@chem.uoa.gr

A. Kalemos
e-mail: kalemos@chem.uoa.gr

recorded its absorption spectrum. He cites spectroscopic parameters and dissociation energies, D_e and D_0, for both the ground ($X\,{}^1\Sigma^+$) and first excited ($a\,{}^3\Pi$), the only "true" bound valence states correlating with ground-state atoms. The accuracy of Wahrhaftig's results for work published more than seventy years ago is indeed remarkable. Table 1 lists, practically, all the experimental structural information for the $X\,{}^1\Sigma^+$ and $a\,{}^3\Pi$ states of ClF concerning the present work (Refs. [4–17]). The work of Schumacher and coworkers published in 1947 and 1950 is not included in Table 1 because of our lack of access to the appropriate journals [18, 19] (see, however, Refs. [6, 7]). It should be mentioned at this point that henceforth the first excited (bound) state, $a\,{}^3\Pi$, will be tagged either A′ (${}^3\Pi_2$), or A (${}^3\Pi_1$), or B (${}^3\mathit{\Pi}_{0^\pm}$), depending on the $\Omega = \Lambda + \Sigma$ value; see footnote (l) of Table 1. If the Ω coupling is not taken into account, the first excited state of ClF will be simply called $a\,{}^3\Pi$ according to standard practice [15].

The first theoretical work on the electronic structure and properties of the X state of ClF was published in 1974 by Staub and McLean [20]. These authors reported Hartree–Fock HF/(DZ + P)—Slater results on all diatomic molecules XX′, X_2, and HX (X = Cl, F, Br, and I). Since then, a significant number of ab initio studies on ClF have been appeared in the literature, the most relevant to the present work given in Refs. [21–27, 31–34][1]. In 1985, Scharf and Ahlrichs [22] performed coupled pair functional (CPF) calculations for the X state of ClF (and ClF_3) employing a $[6s6p/_{\mathrm{Cl}}\ 6s4p/_{\mathrm{F}}]$ + P(olarizaion) basis sets. They report r_e, $D_e + Q$ ($+Q$ = the Davidson correction), and μ_e (equilibrium electric dipole moment). In 1988, Peyerimhoff and coworkers [23] using the multireference single and double excitation MRDCI method (see below) and a Gaussian $[6s5p2d/_{\mathrm{Cl}}\ 4s4p2d/_{\mathrm{F}}]$ + 3s2p bond functions basis set, calculated potential energy curves (PEC) for the first six singlets ($X\,{}^1\Sigma^+$, $1^1\Pi$, $2^1\Pi$, $1^1\Delta$, $1^1\Sigma^-$, $2^1\Sigma^+$), all repulsive except the X state, correlating with Cl(^{2}P) + F(^{2}P). A number of Rydberg and charge transfer states have also been studied. In 1990, Peterson and Woods [24] using the coupled electron pair approximation (CEPA), singles and doubles electron configuration (CISD), and Møller–Plesset fourth-order perturbation theory with single, double, and quadruple excitations (MP4SDQ) combined with a $[12s8p3d1f/_{\mathrm{Cl}}\ 10s3p2d1f/_{\mathrm{F}}]$ Gaussian basis sets, calculated among other things the spectroscopic constants r_e, D_e, ω_e, $\omega_e x_e$, α_e, $\bar{D}_e$, and μ_e of the $X\,{}^1\Sigma^+$ state of the isoelectronic species ClF, ClO^-, SF^-, and ArF^+ around equilibrium. Their results are in good agreement with corresponding experimental numbers. Perera and Bartlett [25] examined the dependence of the electric dipole moments on scalar relativistic effects of the ground states of all six interhalogens XX′ at the coupled cluster level (CCSD) and effective core potentials.

In 1998, de Jong et al. [26] studied the ground states of the six interhalogens XX′ using augmented correlation consistent aug–cc–pVnZ (n = 2, 3) valence basis sets at the MP2, CCSD, and CCSD(T) fully relativistic level of theory. In particular, correlation effects of dipole moments and polarizabilities were obtained through the CISD relativistic approach.

The most systematic and complete theoretical work so far on ClF published in 2000 is that by Alekseyev, Lieberman, and Buenker [27]. These workers performed multireference MRDCI calculations (see Refs. [28–30]) employing relativistic effective core potentials (RECP), treating explicitly the seven valence electrons ($3s^2 3p^5/2s^2 2p^5$) of each halogen atom through a $[7s7p3d1f/_{\mathrm{Cl,F}}]$ basis set. They report full PECs for all 12 $\Lambda - \mathrm{S}$ states correlating with Cl(^{2}P) + F(^{2}P) and five ion pair states, which correlate with the ionic fragments $\mathrm{Cl}^+({}^3\mathrm{P}) + \mathrm{F}^-({}^1\mathrm{S})$. Spin–orbit (SO) effects have been taken into account employing the ${}^{2S+1}\Lambda$ eigenfunctions as basis for the SO calculations. Their results will be compared to ours in due course. Recall, however, that MRDCI calculations involve a specific number of approximations in addition to the RECPs in the present case, details of which are described in Refs. [27–30].

In a mixture of density functional theory DFT(B3LYP) and coupled cluster CCSD(T) calculations combined with aug–cc–pVnZ (n = T, Q, 5) basis sets, Ricca [31] calculated certain ground-state properties of ClF_x (x = 1, 2, 3) around equilibrium. At the highest level of theory including tight d functions and correcting for scalar relativistic and core effects, her ab initio results r_e, D_e, and IE (ionization energy) are in good agreement with experiment. Three years later, Horný et al. [32] reported a series of coupled cluster calculations around equilibrium on the X states of ClF and ClF^- with the purpose of obtaining an accurate value of the electron affinity (EA) of ClF, a controversial quantity indeed (vide infra), using a series of valence cc-pVnZ (n = D, T, Q, 5) basis sets with and without diffuse functions and a variety of coupled cluster (CC) variants (CCSD, CCSD(T), CCSDT, EOM-CC). Besides EA, they predict r_e and ω_e for the neutral species. Their best values at the CCSD(T)/aug–cc–pV5Z level for the $X\,{}^1\Sigma^+$ state of ClF are $r_e = 1.6305$ Å and $\omega_e = 783\ \mathrm{cm}^{-1}$ in agreement with experiment.

Very recently Chen et al. [33] in an effort to understand the bonding in the series of molecules ClF_x (x = 1–7), they performed high-level valence MRCI and CCSD(T) calculations in conjunction with aug–cc–pVnZ (n = T, Q, 5)

---

[1] This just published work by Dunning and coworkers again on ClF_n^+ (n = 1–6) refines the "recoupled pair bonding" model (*rpd*), introduced in order to explain the phenomenon of hypervalency. For another point of view on hypervalency, perhaps more economic and without introducing new models like the rpd, see Refs [35, 36].

Table 1 Experimental results on $^{35}Cl^{19}F$. Bond distances r_e (Å), dissociation energies D_e and D_0 (cm^{-1}), harmonic frequencies and anharmonic corrections ω_e, $\omega_e x_e$, $\omega_e y_e$ (cm^{-1}), rotational vibrational coupling constants α_e (cm^{-1}), electric dipole moments μ_e (D), and separation energies T_e (cm^{-1}) of the $X\ ^1\Sigma^+$ and $a\ ^3\Pi$ states

Footnotes	$X\ ^1\Sigma^+$								
	r_e	D_e[a]	D_0[a]	ω_e	$\omega_e x_e$	$\omega_e y_e$	$\alpha_e \times 10^3$	μ_e	T_e
b	1.625	21,495 ± 3	21,101 ± 2	793.2	9.9		6 ± 2		0.0
c	1.628 (1)		20,633 ± 2	784.1 ± 1	5.3 ± 0.5		4.5 ± 0.4		
d	1.62831						4.359	0.881 ± 0.02	
e			20,406 ± 323						
f								0.8881 (2)	
g			21,108						
h				785.2 ± 1.3	5.3 ± 0.1	−0.03 ± 0.01			
i	1.628341 (4)			783.553 (30)	5.045 (87)		4.325		
j		21,500	21,126 ± 6						
k			21,110 ± 2						
States	$a\ ^3\Pi$[l]								
$^3\Pi_{0^+}$[b]	1.92	2,946 ± 50	2,790 ± 50	313.484	2.217	−0.400	1.4		18,549 ± 50
$^3\Pi_{0^+}$[d]	2.038 (1)			362.4 ± 1	8.8 ± 0.5	−0.14 ± 0.10	3.8 (1)		
$B^3\Pi_{0^+}$[h]				362.5 ± 1.6	8.5 ± 0.4	−0.13 ± 0.03			18,827 ± 4
$B^3\Pi_{0^+}$[j]	2.031[m]	3,079.1		363.1[m]	8.64[m]	−0.124[m]	4.7[m]		18,825.3
$A^3\Pi_1$[k]				353 ± 1	9.7 ± 1	0.17 ± 0.01			18,841 ± 5
$A'^3\Pi_2$[n]	2.0245 (16)	3,243 ± 5		363.53 (2.58)	8.3 (67)		6.31 (28)		18,257 ± 5
$A^3\Pi_1$[o]	2.0247	2,988.4[p]		361.23	7.74		6.28		18,511.6
$B^3\Pi_{0^+}$[o]	2.0221	3,078.7[q]		362.578	8.227		7.36		

[a] With respect to the ground-state atoms including spin–orbit interaction, $Cl(^2P_{3/2}) + F(^2P_{3/2})$

[b] Ref. [4]; ClF absorption spectroscopy; most probable dissociation products of the $^3\Pi_{0^+}$ state are $Cl(^2P_{3/2}) + F(^2P_{3/2})$

[c] Ref. [6]; visible absorption spectrum; D_0 obtained by assuming that the end products of the $^3\Pi$ state are $Cl(^2P_{1/2}) + F(^2P_{3/2})$

[d] Ref. [5]; microwave spectroscopy; r_e calculated from B_e; see also Ref. [3]

[e] Ref. [7]; photoionization study; most probable end products of the $^3\Pi$ state are $Cl(^2P_{1/2}) + F(^2P_{3/2})$. Ionization energy IE[ClF($X\ ^1\Sigma^+$, $v = 0$) → ClF^+ ($X\ ^2\Pi_{3/2}$, $v = 0$)] = 12.65 ± 0.01 eV

[f] Ref. [8]; radio frequency spectroscopy

[g] Ref. [9]; chemiluminescence spectroscopy; end products of the $^3\Pi$ state taken as $Cl(^2P_{3/2}) + F(^2P_{1/2})$

[h] Ref. [10]; emission spectroscopy

[i] Ref. [11]; millimeter rotational spectroscopy

[j] Refs. [12, 13]; laser excitation spectrum; upper limit of D_0 with dissociation products of the B state ($^3\Pi_{0^+}$) taken as $Cl(^2P_{3/2}) + F(^2P_{1/2})$

[k] Ref. [14]; optical–optical double resonance (OODR) spectroscopy; dissociation products of the B state taken as $Cl(^2P_{3/2}) + F(^2P_{1/2})$, $D_0 = 20{,}633\ cm^{-1}$ if end products $Cl(^2P_{1/2}) + F(^2P_{3/2})$

[l] According to standard convention(s) (Ref. [15]; see also Ref. [3]), the first higher state with different spin multiplicity from the ground state of a diatomic molecule (here the first excited state $^3\Pi$) should be named $a\ ^3\Pi$. However, sanctioned by custom the historical naming is followed, that is, A′ ($^3\Pi_2$), A($^3\Pi_1$), and B($^3\Pi_{0^+}$); no letter name has been attached to $^3\Pi_{0^-}$. Unfortunately, this practice is still followed for some historical molecules like N_2, X_2, and XX′

[m] Recalculated in Ref. [3] according to data of Ref. [6]

[n] Ref. [16]; OODR + fluorescence spectroscopy

[o] Ref. [17]; OODR spectroscopy

[p] Ref. [17]; dissociation to two ground-state atoms 21,500 (2) above the X state

[q] Ref. [17]; dissociation to $Cl(^2P_{3/2}) + F(^2P_{1/2})$

basis sets and a tight d function on Cl. For the $X\,^1\Sigma^+$ and $a\,^3\Pi$ states of ClF, their equilibrium structural parameters r_e, D_e (D_0), ω_e, and IE will be contrasted to ours later on.

We turn now to the ClF$^+$ cation. The limited experimental data we are aware of are given in the Huber–Herzberg collection [3], all drawn from Refs. [7, 37–39] published some 40 years ago. The best D_0^0 experimental value of ClF$^+$ ($X\,^2\Pi_{3/2}$) is indirectly obtained through the energy conservation relation $D_0^0(\mathrm{ClF}^+; X^2\Pi_{3/2}) = D_0^0(\mathrm{ClF}; X^1\Sigma^+) + \mathrm{IE}(\mathrm{Cl}; {}^2\mathrm{P}_{3/2}) - \mathrm{IE}(\mathrm{ClF}; X^1\Sigma^+) = 2.617+ 12.96763$ (Ref. [40]) -12.66 (Ref. [3]) eV = 2.924 eV (= 67.43 kcal/mol). The Huber–Herzberg value is D_0^0 = 2.93 eV [3].

There are only two relevant ab initio calculations on ClF$^+$. In 1981, Ewig et al. [21] obtained the vertical ionization energy of ClF within a limited MCSCF-CI/ $[5s4p1d/_{\mathrm{Cl}}\ 4s3p1d/_{\mathrm{F}}]$ approach. Almost 30 years later, Dunning and coworkers [33] reported D_0, r_e, ω_e, of the $X\,^2\Pi$ and $^4\Sigma^-$ states of ClF$^+$ at the valence MRCI (+Q)/ aug–cc–pVnZ (n = T, Q, 5) level. Their best results (MRCI + Q/n = 5) are D_0 = 66.14 (13.08) kcal/mol, r_e = 1.536 (1.1745) Å, and ω_e = 919.9 (363.2) cm^{-1} for the $X\,^2\Pi$ ($^4\Sigma^-$) state. At the MRCI + Q/n = 5 level, the ionization energy is predicted to be IE [ClF($X\,^1\Sigma^+$)→ ClF$^+$($X\,^2\Pi$)] = 12.56 eV, just 0.1 eV less than the experimental value [3].

Hardly anything is known experimentally for the anion ClF$^-$. The four experimental publications that refer to the electron affinity EA, the only (indirectly) measured quantity, seems to be off by more than 0.5 eV (see below). Harland and Thynne [41] are the first to give an EA value of ClF (or the IE of ClF$^-$) after bombarding the pentafluorosulfur chloride with an electron beam; they report EA = 1.5 ± 0.4 eV. Their results were confirmed 10 years later by Dispert and Lacmann [42] who obtained EA = 1.5 ± 0.3 eV. Almost the same time Illenberger et al. [43] through low-energy electron impact experiments on $\mathrm{CF_2Cl_2}$, $\mathrm{CF_3Cl}$, and $\mathrm{CFCl_3}$ concluded that EA (ClF) = 1.79 eV, within the (large) error bars of the previous workers. According to Ref. [32], however, Dudlin et al. [44] "in their electron impact investigation of $\mathrm{ClF_3}$ and its dissociation products estimated the lower limit of $\mathrm{EA_{ad(iabatic)}}$ to be 2.37 ± 0.21 eV". After further analysis of the dissociation energies, the authors suggest that $\mathrm{EA_{ad}}$ = 2.86 ± 0.2 eV (see also Ref. [45]). Obviously, an experimental reinvestigation of the electron affinity of ClF is in order.

We are aware of two ab initio studies on the EA of ClF. Through G3 [46] and G3X [47] calculations, Law et al. [48] report EA = 2.31 and 2.07 eV, respectively. The most recent work on the EA of ClF is that by Horný et al. (vide supra) [32]. Their best results at the CCSD(T)/aug–cc–pV5Z (+zero point energy = ZPE) are $\mathrm{EA_{ad}}$(ClF) = 2.22 (2.25) eV, r_e (ClF$^-$) = 2.1531 Å, and ω_e (ClF$^-$) = 378 cm^{-1}, in harmony with the present work (vide infra).

We believe that the above exposition on the past findings on ClF and ClF$^\pm$ shows the need for a systematic theoretical investigation on these species, confirming or not certain results and reporting new ones. Hence, we have performed highly correlated all electron ab initio calculations via the MRCI, RCCSD(T), and RCCSDT methods combined with large correlation consistent basis sets, including scalar relativistic and core correlation effects on Cl as well as spin–orbit (SO) couplings. The construction of full potential energy curves for a large number of states allows for a better understanding of bonding interactions and the extraction of accurate spectroscopic parameters and energetics. Our work is structured as follows: In Sect. 2, we outline basis sets and methods, Sect. 3 and subsections 3.1, 3.2, and 3.3 refer to results and discussion on ClF, ClF$^+$, and ClF$^-$, respectively, while Sect. 4 epitomizes our general approach and findings.

2 Basis sets and methods

The augmented correlation consistent basis sets of Dunning and coworkers [49–52] for the F and Cl atoms, aug–cc–pVnZ and aug–cc–pV(n + d)Z (n = 5, 6) including a set of tight d functions for Cl were employed in all calculations. Both sets were generally contracted to $[7s6p5d4f3g2h/_{\mathrm{F}}\ 8s7p6d4f3g2h/_{\mathrm{Cl}}]$ and $[8s7p6d5f4g3h2i/_{\mathrm{F}}\ 9s8p7d5f4g3h2i/_{\mathrm{Cl}}]$ for n = 5 (quintuple) and n = 6 (sextuple), renamed for brevity A5ζ and A6ζ and consisting of 263 and 387 spherical Gaussians, respectively. To estimate the core effects on ClF for the Cl atom only ($2s^22p^6$), the A5ζ set was augmented by a series of weighted core functions [53], resulting to $[7s6p5d4f3g2h/_{\mathrm{F}}\ 12s11p9d7f5g3h/_{\mathrm{Cl}}] \equiv$ CA5ζ of order 347. Notice that the CA5ζ basis set does not include the tight d function on Cl. Scalar relativistic valence effects were calculated at the quintuple cardinality level after recontracting the A5ζ basis set accordingly (=A5ζ − rel) [50, 53].

Two methods of correlated calculations are followed, the complete active space self-consistent field + single + double replacements (CASSCF + 1+2 = MRCI), and the (single-reference) restricted coupled cluster + singles + doubles + quasi-perturbative connected triples (RCCSD(T)) [54–57]. The CASSCF reference wavefunctions are defined by allotting 14 (ClF), 13 (ClF$^+$), and 15 (ClF$^-$) electrons to 12 orbitals related to $(3s + 3p/_{\mathrm{Cl}}\ 2s + 2p + 3s + 3p/_{\mathrm{F}})$ atomic orbitals for ClF, ClF$^+$, and ClF$^-$ giving rise to 978, 1,196, and 354 reference configuration functions (CF), respectively. Internally contracted (*ic*) [58, 59], valence MRCI wavefunctions are calculated by single + double excitations out of the CASSCF wavefunctions; of course, all of our reported multireference results are of *ic*MRCI quality. RCCSD(T) valence calculations were performed only for the $X\,^1\Sigma^+$ state of ClF, the $X\,^2\Pi$ and $a\,^4\Sigma^-$ states of ClF$^+$, and the $X^2\Sigma^+$ state of ClF$^-$. In addition, RCCSDT/A5ζ calculations were performed for the X states of ClF, ClF$^+$, and ClF$^-$. Core correlation effects of the $2s^22p^6/_{\mathrm{Cl}}$ electrons are taken into account by including them in the CI and CC procedures, tagged C-MRCI and C-RCCSD(T), respectively. The inclusion of the $2s^22p^6/_{\mathrm{Cl}}$ subvalence electrons in the CI process increases considerably the number of CFs. For instance, the MRCI (*ic*MRCI)/A5ζ expansion of the $X\,^1\Sigma^+$ wavefunction of ClF contains 3.7×10^8 (8.2×10^6) CFs as contrasted to 1.6×10^9 (3.7×10^7) CFs of the C-MRCI(*ic*C-MRCI)/CA5ζ wavefunctions. Corresponding numbers of the (valence) MRCI (*ic*MRCI)/A6ζ are 8.34×10^8 (9.8×10^6) CFs.

Valence scalar relativistic effects for the $X\,^1\Sigma^+$, $a\,^3\Pi$ (ClF), $X\,^2\Pi$, $a\,^4\Sigma^-$ (ClF$^+$), and $X^2\Sigma^+$ (ClF$^-$) were estimated through the Douglas–Kroll–Hess Hamiltonian up to second order (DKH2) [60, 61] using the A5ζ − rel basis set. Spin–orbit effects have been obtained by diagonalizing the $\hat{H}_{\mathrm{el}} + \hat{H}_{\mathrm{SO}}$ Hamiltonian employing the $\hat{H}_{\mathrm{el}}$ MRCI/A5ζ eigenvectors, where $\hat{H}_{\mathrm{SO}}$ is the full Breit–Pauli operator. Basis set superposition errors (BSSE) estimated around equilibrium by the usual counterpoise method [62, 63] are small enough not to be taken into account, for example, for the $X\,^1\Sigma^+$ state of ClF BSSE [MRCI/A5ζ (A6ζ)] = 101 (47) cm^{-1}, with similar results at the CC level. Spectroscopic parameters (r_e, ω_e, $\omega_e x_e$, $\omega_e y_e$, α_e, $\bar{D}_e$) have been determined via the Dunham approach [64, 65]. The number of vibrational levels for certain states was determined by solving numerically the one-dimensional Schrödinger equation of the two nuclei. The size non-extensivity error (SNE) is estimated by subtracting the sum of the energies of the atoms from the energy of the supermolecule at an internuclear distance of 20–30 bohr. We find that for the $X\,^1\Sigma^+$ state of ClF SNE = 8.6 (1.7), 8.7 (1.7) kcal/mol at the MRCI (+Q)/A5ζ or A6ζ level, respectively, where +Q refers to the Davidson correction [66, 67]; see also page 3 of Ref. [68]. Finally, C_{2v} constraints have been imposed through all computations.

The RCCSDT/A5ζ calculations were performed by the CFOUR program [69]; all other calculations were carried out through the MOLPRO 2010 package [70].

3 Results and discussion

3.1 ClF

For reasons of convenience, Table 2 lists the most reliable, according to the present authors, experimental values of the $X\,^1\Sigma^+$ and $B\,^3\Pi_{0^+}$ states of ^{35}Cl^{19}F; see also Table 1. The interaction of the ground-state atoms Cl(^{2}P) + F(^{2}P) gives rise to 12 molecular $^{2S+1}\Lambda$ states, singlets and triplets, that is, ^{1,3}(Σ^+[2], Σ^-, Π[2], Δ). Two of them $X\,^1\Sigma^+$ and $a\,^3\Pi$ are bound, one is a *van der Waals* state ($1^1\Pi$), whereas the rest of the nine states are strongly repulsive. For all 12 states, full MRCI + Q/A5ζ PECs are displayed in Fig. 1. The second adiabatic channel Cl ($3s^23p^44s^1$; ^{4}P) + F(^{2}P) located 8.922 eV higher gives rise to states of Rydberg character; the third and fourth channels are of charge transfer nature, Cl$^+$(^{3}P) + F$^-$(^{1}S) and Cl$^+$(^{1}D) + F$^-$(^{1}S), located 9.566 and 11.011 eV above the X state, respectively [71]. From the third and fourth channels, five ion pair states (Cl$^+$F$^-$) of $^3\Sigma^-$, $^3\Pi$ and $^1\Sigma^+$, $^1\Pi$, and $^1\Delta$ symmetry emerge. We note that the F$^-$ anion does not have any excited states (vide infra). As was already mentioned, the present study deals exclusively with the first 12 valence $\Lambda - S$ states related to the first Cl(^{2}P) + F(^{2}P) channel.

Table 2 "Best" experimental properties of the $X\,^1\Sigma^+$ and $B^3\Pi_{0^+}$ states of ^{35}Cl^{19}F according to Table 1. Apart from r$_e$ (Å) and μ$_e$ (Debye) all units are in cm^{-1}

Properties	$X\,^1\Sigma^+$	$B^3\Pi_{0^+}$
r_e	1.628341 (4)	2.0221
D_e^0	21,500[a]	3078.7[c]
D_0^0	21,110[b]	
ω_e	783.353	362.6
$\omega_e x_e$	5.045	8.3
$\omega_e y_e$	−0.003 (1)	
$\alpha_e \times 10^3$	4.325	7.4
$\bar{D}_e \times 10^7$	8.98[d]; 8.77[e]	11.0[f]
μ_e	0.8881 (2)	
T_e	0.0	18,825.3

[a] 2.666 eV = 61.47 kcal/mol

[b] 2.616 eV = 60.36 kcal/mol

[c] 0.3817 eV = 8.802 kcal/mol

[d] Refs. [12, 13]

[e] Calculated through $\bar{D}_e = 4B_e^3/\omega_e^2$ where B_e and ω_e are taken from Refs. [4, 5], respectively; see also Ref. [3]

[f] Obtained by us using the B_e and ω_e given in Refs. [12, 13]

3.1.1 $X\,^1\Sigma^+$

Table 3 lists our numerical results on the $X\,^1\Sigma^+$ state of ClF, whereas Fig. 1 displays all 12 MRCI + Q/A5ζ $^{2S+1}\Lambda$ PECs correlating with the ground-state atoms. The bonding of the $X\,^1\Sigma^+$ state is described succinctly by the valence-bond-Lewis (vbL) diagram shown below along with the leading equilibrium MRCI/A5ζ CFs (only valence e$^-$ are counted).

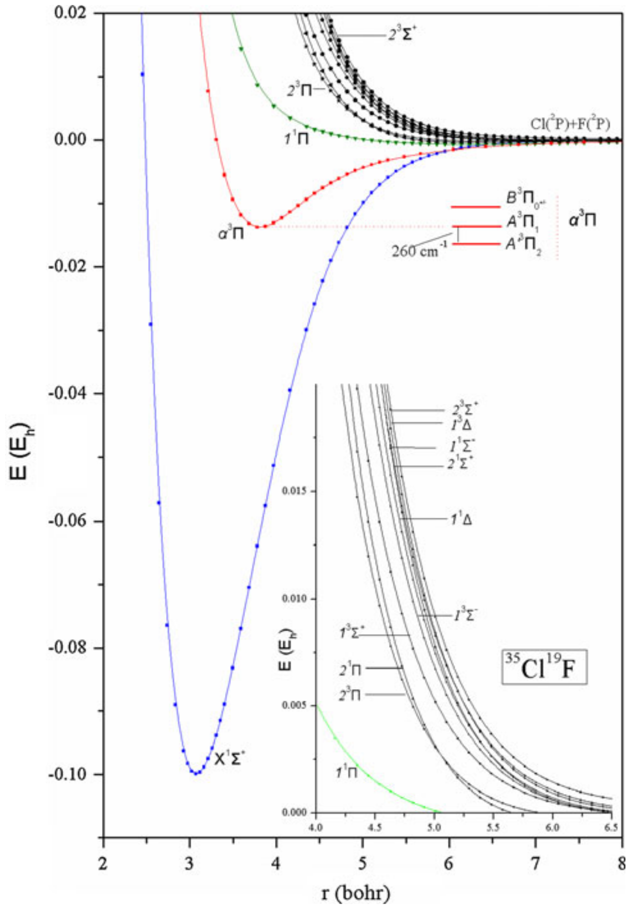

Fig. 1 Relative MRCI + Q/A5ζ PECs of twelve $^{2S+1}\Lambda$ valence states of ClF correlating with Cl(^{2}P) + F(^{2}P). Two states are bound ($X\ ^1\Sigma^+$, $a\ ^3\Pi$), one is of vdW nature ($1^1\Pi$) and the rest strongly repulsive. The first *inset* magnifies the nine repulsive PECs, and the second shows the Ω splittings of the $a\ ^3\Pi$ state

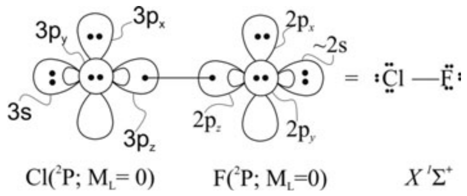

$$|X^1\Sigma^+\rangle \approx \left|1\sigma^2 2\sigma^2[(0.94)3\sigma^2 - (0.11)4\sigma^2]1\pi_x^2 1\pi_y^2 2\pi_x^2 2\pi_y^2\right\rangle.$$

According to the Mulliken population analysis, a total charge of 0.25 e$^-$ is transferred from Cl to F, resulting to a Cl$^+$F$^-$ charge polarity. All our results listed in Table 3, with the exception of the second anharmonicity $\omega_e y_e$, are in very good agreement with experiment. The MRCI + Q/A6ζ and RCCSD(T)/A6ζ properties corrected for core ($2s^2 2p^6$/$_{\text{Cl}}$) and scalar relativistic effects, employing the CA5ζ and A5ζ − rel basis sets at the corresponding methods, are referred as "best" values; Table 3. For instance, at the CC level r_e ("best") ≡ $r_e^* = r_e$ [RCCSD(T)/A6ζ] + $\delta r_{\text{core}} + \delta r_{\text{rel}}$ where, $\delta r_{\text{core}} = r_e$ [C-RCCSD(T)/CA5ζ] − r_e [RCCSD(T)/A5ζ] and $\delta r_{\text{rel}} = r_e$[RCCSD(T) + DK/A5ζ − rel] − r_e [RCCSD(T)/A5ζ]. Therefore, $r_e^* = 1.6289 + (-0.0022) + 0.0017 = 1.6284$ Å in perfect agreement with experiment; Table 3. Exactly the same r_e^* (=1.6284 Å) is obtained at the MRCI + Q level. Dissociation D_e^* values are 62.78 (MRCI) and 62.21 (RCCSD(T)) kcal/mol with respect to Cl(^{2}P) + F(^{2}P). Taking into account, however, the calculated (experimental [71]) SO splitting $\Delta E(^2P_{3/2} - {}^2P_{1/2}) = 799.1$ (881) and 398.1 (404) cm^{-1} for Cl and F, respectively, the dissociation energy D_e with respect to the lowest Cl($^2P_{3/2}$) + F($^2P_{3/2}$) fragments and disregarding the SO effects of the X $^1\Sigma^+$ state as negligible (~5 cm^{-1}), is D_e^0(MRCI + Q) = $D_e^* - 1/3 \times \Delta E_{\text{Cl}}(^2P_{3/2} - {}^2P_{1/2}) - 1/3 \times \Delta E_{\text{F}}(^2P_{3/2} - {}^2P_{1/2}) = 62.78$ kcal/mol − 1/3 × 799.1 cm^{-1} − 1/3 × 398.1 cm^{-1} = 61.64 kcal/mol. Also D_0(MRCI + Q) = D_e^0(MRCI + Q) − $\omega_e/2 + \omega_e x_e/4$ = 61.64 kcal/mol − 787.7/2 cm^{-1} + 4.70/4 cm^{-1} = 60.35 kcal/mol. Analogously, the CC method gives D_e^0[RCCSD(T)] = 62.21 kcal/mol − 1/3 × 799.1 cm^{-1} − 1/3 × 398.1 cm^{-1} = 61.07 kcal/mol. The MRCI + Q D_e (D_0) = 61.64 (60.35) kcal/mol can be considered as in perfect agreement with the experimental value of 61.47 (60.35) kcal/mol (see Table 3), while the CC value is by 0.40 kcal/mol smaller. Corresponding numbers from Ref. [27] are $r_e = 1.641$ Å and $D_e^0 = 58.62$ kcal/mol. Notice that at the CC/A5ζ level triple excitations either perturbatively (RCCSD(T)) or self-consistently (RCCSDT) give identical results; see Table 3. Spectroscopic constants ω_e^*, $\omega_e x_e^*$, α_e, and $\bar{D}_e$ are in very good agreement with the experimental results as well.

We now turn to the permanent electric dipole moment of the X $^1\Sigma^+$ state of ClF. All calculated values listed in Table 3 either MRCI + Q or CC have been obtained through the finite field approach; see also Ref. [72]. The μ_e^*[RCCSD(T)] = 0.891 D is in complete agreement with the experimental value ($\mu_e = 0.8881(2)$ D), while μ_e^*[MRCI + Q] = 0.865 D is smaller by 0.023 D, a relative error of less than 3 %. It is interesting to note that in 1973 Flygare et al. [73, 74] reported an experimental value $\mu_e = 2.1 \pm 1.4$ D and an opposite charge polarity, Cl–F$^+$. The latter was challenged very soon by Green [75] whose CI calculations indicated the reverse polarity and confirmed "experimentally" to be indeed Cl$^+$F$^-$ by Janda et al. [76] and Fabricant and Muenter [77]. For a similar misunderstanding concerning the polarity of boron monofluoride (BF), see Ref. [78] and references therein.

Table 3 Total energies E (E_h), bond distances r_e (Å), dissociation energies D_e (kcal/mol), harmonic frequencies ω_e (cm^{-1}), anharmonicities $\omega_e x_e$ and $\omega_e y_e$ (cm^{-1}), rotational vibrational coupling constants α_e (cm^{-1}), centrifugal distortions $\bar{D}_e$(cm^{-1}), and dipole moments μ_e (D) of the $X\ ^1\Sigma^+$ state of ^{35}Cl^{19}F at the MRCI + Q (MRCI), RCCSD(T) and RCCSDT methods. Previous theoretical and experimental results are given for easy comparison

Method	$-E$	r_e	D_e^a	ω_e	$\omega_e x_e$	$\omega_e y_e$	$\alpha_e \times 10^3$	$\bar{D}_e \times 10^7$	μ_e^b
MRCI + Q/A5ζ	559.45806	1.6279	62.79	789.4	5.18	−0.109	4.32	8.86	0.879
MRCI + Q/A6ζ	559.46375	1.6263	62.99	789.5	5.63	0.068	4.64	8.90	0.870
(MRCI/A6ζ)[c]	(559.43428)	(1.6234)	(62.83)	(797.8)	(6.24)	(0.04)	(4.64)	(8.83)	(0.897)
C-MRCI + Q/CA5ζ	559.79451	1.6281	63.01	788.4	4.85	−0.029	4.24	8.89	0.865
MRCI + DK + Q/A5ζ − rel	560.95509	1.6298	62.36	787.0	5.62	0.008	4.50	8.86	0.892
"Best" values[d]		1.6284	62.78	786.1	5.74				0.871
RCCSD(T)/A5ζ	559.46165	1.6299	62.22	791.8	4.97	−0.026	4.22	8.79	0.875
RCCSDT/A5ζ	559.46200	1.6306	61.72	788.2					
RCCSD(T)/A6ζ	559.46760	1.6289	62.49	790.0	4.85	−0.026	4.21	8.82	0.876
C-RCCSD(T)/CA5ζ	559.80680	1.6277	62.25	791.3	4.77	−0.099	4.04	8.83	0.872
RCCSD(T) + DK/A5ζ − rel	560.95866	1.6316	61.91	790.0	5.02	−0.012	4.24	8.78	0.893
"Best" values[d]		1.6284	62.21	787.7	4.70				0.891
MRD − CI[e]		1.641	59.70	785					
MRCI + Q/A5ζ[f]	559.45004	1.627	60.18	797.8					
CCSD(T)[f]	559.46165	1.629	62.21	788.2					
Expt.[g]		1.628341 (4)	61.47	783.353	5.045	−0.003	4.325	8.77	0.8881

[a] With respect to the ground-state atoms Cl(^{2}P) + F(^{2}P)

[b] Calculated by the finite field approach; fixed strength 5 × 10^{-5} a.u.

[c] MRCI/A6ζ values (no +Q correction) given for comparison

[d] Corrected MRCI + Q/A6ζ and RCCSD(T)/A6ζ values for core and scalar relativistic effects at the CA5ζ and A5ζ − rel levels of theory; see text

[e] Ref. [27]

[f] Ref. [33]

[g] See Table 2

3.1.2 *a* $^3\Pi$

Figure 1 displays the MRCI + Q/A5ζ PEC of the $a\ ^3\Pi$ state, while Table 4 lists numerical results corrected for scalar relativistic effects ("best" values). To avoid large relative errors that could possibly be induced by the +Q Davidson correction when treating 14 (valence) + 8 (core) = 22 electrons by the MRCI method (see below) for a state of less than 10 kcal/mol binding energy like the $a\ ^3\Pi$ one, core corrections are not included. Within the $^{2S+1}\Lambda$ ansatz, the $a\ ^3\Pi$ state is the first and only excited bound state of ClF correlating with Cl(^{2}P) + F(^{2}P). Its bond strength and distance, however, are much weaker and much longer, respectively, than those of the $X\ ^1\Sigma^+$ state. Clearly, two end combinations Cl(^{2}P; $M = 0$) + F(^{2}P; $M = \pm1$) or Cl(^{2}P; $M = \pm1$) + F(^{2}P; $M = 0$) result to two states of $^3\Pi$ symmetry. According to the Mulliken population analysis, the $a\ ^3\Pi$ state correlates with the first one ($M = 0, \pm1$), whereas the repulsive $2^3\Pi$ state (see Fig. 1) correlates with the second ($M = \pm1, 0$) combination. The vbL bonding diagram, leading equilibrium MRCI configurations, and Mulliken atomic populations at r_e and r_∞(20 bohr) of the $a\ ^3\Pi$ state are given below

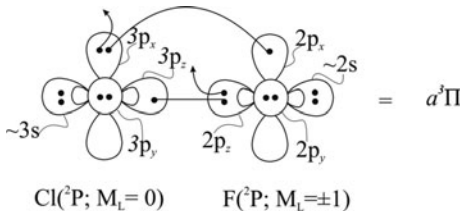

$$|a^3\Pi\rangle \approx \left|1\sigma^2 2\sigma^2 3\sigma^2 4\sigma^1 [(0.79) 1\pi_x^2 2\pi_x^1 - (0.32) 1\pi_x^1 2\pi_x^2] 1\pi_y^2 2\pi_y^2\right\rangle$$
$$- 0.35\left|1\sigma^2 2\sigma^2 3\sigma^1 4\sigma^2 1\pi_x^2 2\pi_x^1 1\pi_y^2 2\pi_y^2\right\rangle$$

$$\mathrm{r_e} : 3s^{1.97} 3p_z^{1.50} 3p_x^{1.23} 3p_y^{1.97} /_{\mathrm{Cl}} 2s^{1.98} 2p_z^{1.46} 2p_x^{1.73} 2p_y^{1.98} /_{\mathrm{F}}$$
$$\mathrm{r_\infty} : 3s^{1.98} 3p_z^{1.03} 3p_x^{1.94} 3p_y^{1.97} /_{\mathrm{Cl}} 2s^{1.98} 2p_z^{1.96} 2p_x^{1.03} 2p_y^{1.99} /_{\mathrm{F}}$$

The vbL icon indicates that the $M = 0$ (Cl) + $M = \pm1$ (F) combination leading to two 3e$^-$ − 2c(enter) interaction

Table 4 Total energies E (E_h), bond distances r_e (Å), dissociation energies D_e (kcal/mol), harmonic frequencies ω_e (cm^{-1}), anharmonicities $\omega_e x_e$ and $\omega_e y_e$ (cm^{-1}), rotational vibrational coupling constants α_e (cm^{-1}), centrifugal distortions $\bar{D}_e$(cm^{-1}), dipole moments μ_e (D), and energy separations T_e (cm^{-1}) of the $a\ {}^3\Pi$ state of $^{35}Cl^{19}F$ at the MRCI + Q method. Previous theoretical and experimental results are given for comparison

Method	$-E$	r_e	D_e^a	ω_e	$\omega_e x_e$	$\omega_e y_e$	$\alpha_e \times 10^3$	$\bar{D}_e \times 10^7$	μ_e^b	T_e
MRCI + Q/A5ζ	559.37191	2.0159	8.70	364.4	9.92	−0.265	6.94	11.5	1.618	18,908
MRCI + Q/A6ζ	559.37720	2.0144	8.70	365.3	10.3	−0.173	7.14	11.5	1.567	18,996
(MRCI/A6ζ)^c	(559.345460)	(2.0293)	(6.91)	(334.7)	(11.8)	(−0.163)	(8.49)	(13.17)	(1.550)	(19,494)
MRCI + DK + Q/A5ζ − rel	560.86954	2.0160	8.75	365.5	10.1	−0.212	7.04	11.5	1.634	18,776
“Best” values^d		2.0145	8.75	366.6	10.5				1.583	18,864
MRD − CI^e		2.064		∼350						
MRCI + Q/A5ζ^f	559.36168	2.072	4.73	250						19,393
Expt.^{g}		2.0221	8.802	362.6	8.3					18,825.3

[a] With respect to the ground-state atoms Cl(^{2}P) + F(^{2}P)

[b] Calculated by the finite field approach; fixed strength 5×10^{-5} a.u.

[c] MRCI/A6ζ values (no +Q correction) given for comparison

[d] Corrected MRCI + Q/A6ζ values for core and scalar relativistic effects only; see text

[e] Ref. [27]

[f] Ref. [33]

[g] Results for the $B^3\Pi_{0^+}$ state; see Table 2 and text

is not conducive for strong bonding, rather the opposite, hence the weak binding and considerable bond lengthening as compared to the $X\ {}^1\Sigma^+$ state. The population distribution suggests that ∼0.5 e$^-$ migrate from F to Cl along the σ frame with a concomitant back transfer from Cl to F of ∼0.7 e$^-$ along the π frame, resulting to the Cl^+F^- polarity with the in situ F atom negatively charged by ∼0.2 e$^-$.

From Table 4, we can see the excellent agreement at all levels of theory but the MRCI/A6ζ, due to SNE effects (no +Q amendment), and that relativistic effects are very small. Recall that we are working within the $\Lambda - S$ frame and that the experimental data cited in Table 4 refer to the B ($^3\Pi_{0^+}$) Ω component of the $a\ {}^3\Pi$ multiplet (see below). Experiment and theory are in excellent harmony, the absolute differences ΔX from the “best” listed values X_e*, $\Delta X = |X_{expt} - X_e^*|$, being $\Delta r_e = 0.008$ Å, $\Delta D_e = 0.05$ kcal/mol, $\Delta\omega_e = 4.0$ cm^{-1}, $\Delta\omega_e x_e = 2.2$ cm^{-1}, $\Delta\alpha_e \sim 0.3 \times 10^{-3}$ cm^{-1}, $\Delta\bar{D}_e = 0.5 \times 10^{-7}$ cm^{-1}, and $\Delta T_e = 39$ cm^{-1}. The electric dipole moment of the $a\ {}^3\Pi$ state is experimentally unknown, determined theoretically for the first time in the present work; the recommended calculated finite field value is $\mu_e = 1.62 \pm 0.02$ D. Corresponding ΔX differences from Ref. [27] are $\Delta r_e = 0.021$ Å, $\Delta\omega_e = 10.1$ cm^{-1}, and $\Delta T_e = 379$ cm^{-1}; no μ_e or D_e^0 values are given.

Before we turn to the Ω states, a word of caution is needed as to the RCCSD(T) calculations of the $a\ {}^3\Pi$ state. Its strong multireference character precludes the use of a single-reference CC method. Indeed, our RCCSD(T)/A5ζ calculations around equilibrium gave results of questionable reliability; that’s why they are not included in Table 4. See also the CCSD(T) numbers on the $a\ {}^3\Pi$ state of Chen et al. [33].

Taking into account the $\Omega = \Lambda + \Sigma$ coupling, the $a\ {}^3\Pi$ state splits into $^3\Pi_2$, $^3\Pi_1$, and $^3\Pi_{0^\pm}$, where to a first approximation the energy separation between the Ω components is given by $\Delta T = A\Lambda\Sigma$, A = constant for a given multiplet. For $\Lambda \neq 0$ as in the present case, however, second-order interactions split slightly the $\Omega = 0$ component into 0^+ and 0^-. In the present case, our calculations do not allow for a 0^+ to 0^- separation; therefore, within our approach, the $^3\Pi_{0^\pm}$states can be identified with the $^3\Pi_0$.

The A′ $^3\Pi_2$ state is lower in energy (inverted), the calculated MRCI + Q/A5ζ SO $\Delta T(^3\Pi_{0^\pm} - {}^3\Pi_1, {}^3\Pi_1 - {}^3\Pi_2)$ being equidistant with $\Delta T = 260$ cm^{-1}, therefore $A = 260$ cm^{-1}; see the upper inset of Fig. 1. Experimentally, it is found that $\Delta T = 255$ [12, 13, 17] and 313 cm^{-1} (Ref. [16]) for the $\Omega = 0^+ - 1$ and 1–2 splittings, respectively. The 0^+ to 0^- separation has not been determined experimentally, but according to the MRDCI calculations of Buenker and coworkers [27], the 0^- component lies below the 0^+ by ∼27 cm^{-1}, a rather large number for this kind of splitting. At the MRCI + Q/A5ζ level of theory, the bond distances of the $^3\Pi_{0^\pm}$, $^3\Pi_1$, and $^3\Pi_2$, states are (experimental values for B, A, and A′ states in parenthesis), $r_e = 2.0245$ (2.0221 or 2.031), 2.0233 (2.0247), and 2.0221 (2.0245) Å, respectively (see Tables 1 and 2). Observe that the absolute differences between experiment and theory are not larger than 0.002 Å.

3.1.3 $1^1\Pi$

The $1^1\Pi$ state is in essence repulsive; its PEC however presents a shallow minimum of less than 0.5 kcal/mol at $r_e \sim 3.3$ Å, so it can be characterized as a *van der Waals* (vdW) state; see Fig. 1. It correlates with the $M = 0$ (Cl) + $M = \pm 1$ (F) projections of the ground-state atoms. Around 3.3 Å, there are two leading MRCI configurations of almost equal weight

$$\begin{aligned}\left|1^1\Pi\right\rangle \approx\ & 0.69\left|1\sigma^2 2\sigma^2 3\sigma^1 4\sigma^2 1\pi_x^2 1\pi_y^2 2\bar{\pi}_x^1 2\pi_y^2\right\rangle \\ & + 0.64\left|1\sigma^2 2\sigma^2 3\sigma^2 4\sigma^1 1\bar{\pi}_x^1 1\pi_y^2 2\pi_x^2 2\pi_y^2\right\rangle\end{aligned}$$

At the MRCI + Q/A6ζ level of theory r(vdW) = 3.31 Å (=6.25 bohr), ΔE(vdW) = −0.43 kcal/mol (= −150 cm^{-1}), $\omega = 44$ cm^{-1}, and $T(1^1\Pi \leftarrow X\ ^1\Sigma^+) = 21{,}795$ cm^{-1}. Interestingly enough the well depth of 150 cm^{-1} can sustain six vibrational levels. At the MRDCI level, Buenker and coworkers predicted a well depth of ~100 cm^{-1} at *r*(vdW) ~6.5 bohr [27].

3.1.4 Repulsive states

Nine more $^{2S+1}\Lambda$ valence states all of strong repulsive character correlate with the ground-state atoms Cl(^{2}P) + F(^{2}P), namely $2^3\Pi$, $2^1\Pi$, $1^3\Sigma^+$, $1^3\Sigma^-$, $1^1\Delta$, $2^1\Sigma^+$, $1^1\Sigma^-$, $1^3\Delta$, and $2^3\Sigma^+$, all calculated at the MRCI + Q/A5ζ level; see lower inset of Fig. 1. The two states of the same spatial–spin symmetry, $1^3\Sigma^+$ and $2^3\Sigma^+$, do not seem to interact at this level, while at distances shorter than 4.5 bohr the energy ordering is the one given above and shown in Fig. 1. Crossings of the pairs $2^1\Sigma^+ - 1^1\Sigma^-$, $2^3\Pi$–$2^1\Pi$, $2^1\Sigma^+ - 1^3\Delta$, and $1^1\Delta$–$1^1\Sigma^-$ are observed at distances ~4.5, 5.0, 5.1, and 5.3 bohr, respectively.

3.2 ClF$^+$

It is useful to collect at this point all we know experimentally on ClF$^+$: $D_0^0 = 67.43$ kcal/mol (see the Sect. 1), ω_e ($X\ ^2\Pi_{3/2}$, $^2\Pi_{1/2}$) = 870 or 912 ± 30 cm^{-1}, SO splitting $\Delta E_{SO} = 630$ cm^{-1}, and IE[ClF($X\ ^1\Sigma^+$)→ClF$^+$($X\ ^2\Pi_{3/2}$)] = 12.66 eV [3]; see also Refs. [38, 39]. In comparison with the $X\ ^1\Sigma^+$ state of ClF, the D_0^0 of ClF$^+$ is 7.1 kcal/mol larger.

The IEs of Cl and F are 12.96763 [40] and 17.42282 eV [79], respectively. The ground state of Cl$^+$ is ^{3}P ($3s^23p^4$) with the first ^{1}D ($3s^23p^4$), second ^{1}S ($3s^23p^4$), and third ^{3}P($3s^13p^5$) excited states 1.402, 3.414, and 11.57 eV higher, respectively [71]. Thus, the adiabatic dissociation products of the first three channels are Cl$^+$(^{3}P, ^{1}D, ^{1}S) + F(^{2}P). We have constructed all 12 doublets and quartets PECs from the first channel Cl$^+$(^{3}P) + F(^{2}P), $^{2,4}(\Sigma^+, \Sigma^-[2], \Pi[2], \Delta)$, all nine doublets from the second channel Cl$^+$(^{1}D) + F(^{2}P) → $^2(\Sigma^+[2], \Sigma^-, \Pi[3], \Delta[2], \Phi)$, and the two doublets $^2\Sigma^+$ and $^2\Pi$ correlating with the third channel Cl$^+$(^{1}S) + F(^{2}P), a total of 23 states. Figure 2 displays the 21 PECs correlating adiabatically with the first two channels; the two highest PECs ($^2\Sigma^+$, $^2\Pi$) originating from the third channel are not shown (but see below). Table 5 lists our theoretical results for the $X\ ^2\Pi$, $a\ ^4\Sigma^-$, $2^2\Pi$, and $3^2\Pi$ states along with available experimental and theoretical results by Dunning and coworkers [33] for the first two states. Notice that at the same level of theory, MRCI + Q/A5ζ, the total energies of the $X\ ^2\Pi$ and $a\ ^4\Sigma^-$ states are lower in the present calculations by 6.4 and 8.3 mE_h, respectively, as compared to Ref. [33]; see Table 5. The reason is the extended zero-order space used here; see Sect. 2.

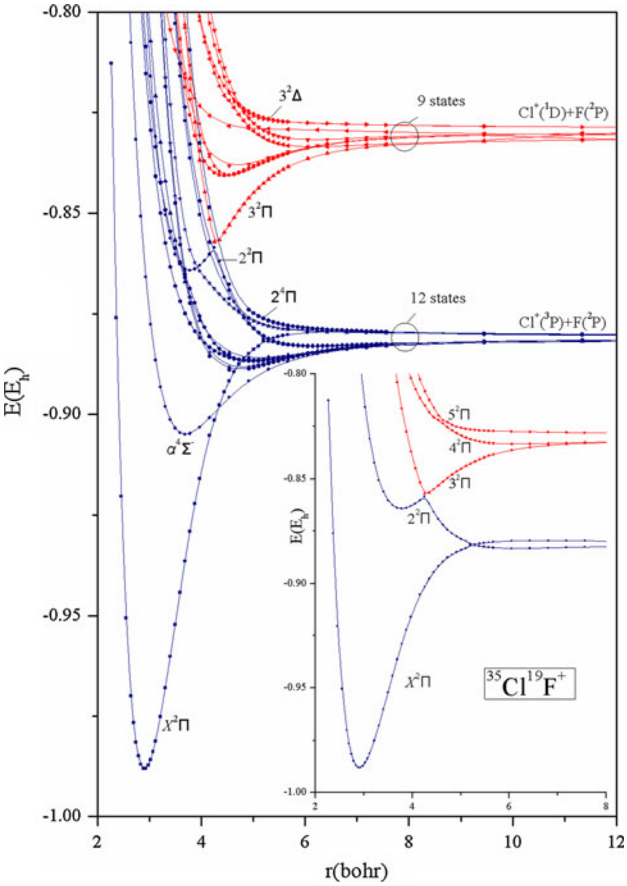

Fig. 2 Relative MRCI + Q/A5ζ PECs of twelve (*first channel*) and nine (*second channel*) states of ClF$^+$. The *inset* displays the avoided crossing among the $^2\Pi$ states

Table 5 Total energies E (E_h), bond distances r_e (Å), dissociation energies D_e and D_0 (kcal/mol), harmonic frequencies ω_e (cm^{-1}) and anharmonicities $\omega_e x_e$ (cm^{-1}), rotational vibrational coupling constants α_e (cm^{-1}), ionization energies IE (eV), and energy separations T_e (cm^{-1}) of the $X\,^2\Pi$, $a\,^4\Sigma^-$, 2 $^2\Pi$ and $3^2\Pi$ bound states of $^{35}Cl^{19}F^+$

Method	$-E$	r_e	D_e[a]	D_0[a]	ω_e	$\omega_e x_e$	$\alpha_e \times 10^3$	IE	T_e
$X\,^2\Pi$									
MRCI + Q/A5ζ	558.99504	1.5367	68.35	67.05	911.7	5.78	5.0	12.61	0.0
MRCI + Q/A6ζ	559.00034	1.5357	68.70	67.40	913.7	5.86	5.0	12.61	0.0
RCCSD(T)/A5ζ	559.99515	1.5358	68.10	66.78	929.5	5.58	4.8	12.69	0.0
RCCSD(T)/A6ζ	559.00065	1.5349	68.16	66.83	931.7	5.99	4.8	12.71	0.0
RCCSDT/A5ζ	558.99686	1.5365	68.08		936.6			12.66	
MRCI + Q/A5ζ[b]	558.98865	1.536	67.44	66.14	911.9				
Expt.		1.53[d]		67.43[c]	870[d], 912[e]			12.66[d,e,f]	0.0
$a\,^4\Sigma^-$									
MRCI + Q/A5ζ	558.91059	1.9491	16.05[a]	15.50[a]	397.1	11.8	2.9		18,535
MRCI + Q/A6ζ	558.91537	1.9475	16.10	15.54	398.5	11.9	2.5		18,649
MRCI + Q/A5ζ[b]	558.90233	1.9745	13.59	13.07	363.2				18,945
2 $^2\Pi$[g]									
MRCI + Q/A5ζ	558.86428	2.00	20.6	20.0	410	4.5		16.15	28587
Expt.[h]								16.39 (1)	
3 $^2\Pi$[i]									
	558.8574	~2.27	~16	15	~725			~16	~30,200

[a] Dissociation energies with respect to the adiabatic products $Cl^+(^3P) + F(^2P)$ for the $X\,^2\Pi$ and $a\,^4\Sigma^-$ states. $D_0 = D_e - \omega_e/2 + \omega_e x_e/4$

[b] Ref. [33].

[c] See introduction and Ref. [3]. This value refers to $X\,^2\Pi_{3/2}$

[d] Ref. [39]

[e] Ref. [38]

[f] With respect to $X\,^2\Pi_{3/2}$

[g] The $2^2\Pi$ is the lowest state correlating diabatically with the second energy channel $Cl^+(^1D) + F(^2P)$. D_e with respect to the diabatic products (second channel)

[h] Ref. [38]; IE = $[E(2^2\Pi) - E(X\,^1\Sigma^+)] + \Delta\omega_e/2$/MRCI + Q/A5ζ

[i] Pseudostate; see tex

3.2.1 $X\,^2\Pi$

The lowest state of ClF$^+$ is certainly of $^2\Pi$ symmetry correlating with $Cl^+(^3P) + F(^2P)$. The vbL icon describing the bonding of ClF$^+$ is that of the $X\,^1\Sigma^+$ state of ClF after removing one electron from a $3p_\pi$ atomic (or 2π molecular) orbital of the neutral species and of course with similar leading configurations. The calculated MRCI + Q/A5ζ or A6ζ (RCCSD(T)/A6ζ) ionization energy of ClF($X\,^1\Sigma^+$) is IE = 12.61 (12.71) eV, in excellent agreement with experiment (IE = 12.66 eV [38, 39]; Table 5). Recall that IE(Cl) = 12.97 eV [40], hence the electron is removed from the chlorine atom in ClF. According to the Mulliken analysis, upon bonding the charge distribution is $^{+0.90}Cl - F^{+0.10}$.

According to Table 5, the bond distance of ClF$^+$ ranges between 1.5349 (RCCSD(T)/A6ζ) and 1.5367 (MRCI + Q/A5ζ) Å. Core and relativistic effects are quite small changing slightly the bond distance and the binding energy. At the MRCI + Q/A5ζ (RCCSD(T)/A5ζ) core and special relativity are responsible for $\delta r_{core} + \delta r_{rel} = -0.0034$ (-0.0031) + 0.0018 (0.0016) Å = -0.0016 (-0.0015) Å. Therefore, our "best" MRCI + Q(RCCSD(T))/A6ζ bond length is $r_e{*}$ = 1.5357–0.0016 (1.5349–0.0015) = 1.5341 (1.5334) Å, both values in agreement with the 1.536 Å of Ref. [33]. The experimental r_e value of ClF$^+$ has been estimated to be 0.1 Å less than that of ClF($X\,^1\Sigma^+$) [32], therefore r_e(expt) = 1.628–0.1 ≈ 1.53 Å, in pleasant agreement with the present calculated value(s).

Combined core and relativistic effects increase (decrease) the dissociation energy D_e by 0.49 (0.59) kcal/mol at the MRCI + Q (RCCSD(T))/A5ζ level of theory. Therefore, our "best" MRCI + Q (RCCSD(T))/A6ζ dissociation energy is (see Table 5), $D_e{*}$ = 68.70 + 0.49 (68.16–0.59) = 69.19 (67.57) kcal/mol, or $D_0{*}$ = 67.89 (66.21) kcal/mol for the $X\,^2\Pi$ state of ClF$^+$. The experimental $D_0 = 67.43$ kcal/mol given in Table 5 refers to the $\Omega = 3/2$ component of the $X\,^2\Pi$ state. Taking into account the SO splitting of both the ClF$^+$ species and the Cl$^+$ and F atoms, our final MRCI + Q (RCCSD(T))/A6ζ D_0 value of the $X\,^2\Pi_{3/2}$ state of ClF$^+$ is $D_0 = D_0^* + 1/2 \times \Delta E_{\mathrm{ClF}^+}({}^2\Pi_{3/2} - {}^2\Pi_{1/2}) - 1/3 \times \Delta E_{\mathrm{F}}({}^2\mathrm{P}_{3/2} - {}^2\mathrm{P}_{1/2}) - 1/9 \times \Delta E_{\mathrm{Cl}^+}({}^3\mathrm{P}_0 - {}^3\mathrm{P}_2) - 3/9 \times \Delta E_{\mathrm{Cl}^+}({}^3\mathrm{P}_1 - {}^3\mathrm{P}_2) = 67.89$ (66.21) kcal/mol + {1/2 × 630 − 1/3 × 404 − 1/9 × 996 − 3/9 × 697} cm^{-1} = 67.42 (65.74) kcal/mol, where experimental SO splittings have been used. In particular, the experimental $\Delta E_{\mathrm{ClF}^+}({}^2\Pi_{3/2} - {}^2\Pi_{1/2})$ SO splitting is 628 ± 30 [38] or 630 ± 30 [39] cm^{-1}, with the $^2\Pi_{3/2}$ being the lower component; the corresponding calculated splitting is 607 cm^{-1}. Obviously the agreement with experiment is excellent, the difference being −0.01 kcal/mol (=−3.5 cm^{-1}) at the MRCI + Q level of theory, but at the RCCSD(T) level the discrepancy is +1.69 kcal/mol (=591 cm^{-1}). As previously reported, RCCSDT/A5ζ results corroborate completely the RCCSD(T)/A5ζ values; see Table 5.

As a final word for the $X\,^2\Pi$ state, it can be said that our results suggest that the experimental harmonic frequency ω_e is closer to 912 cm^{-1} rather than to 870 cm^{-1}; see Table 5.

3.2.2 *a* $^4\Sigma^-$

This is the first excited state of ClF$^+$, a rather dark state for the experimentalists being spin and Franck–Condon forbidden; no experimental results are available. The $a\,^4\Sigma^-$ state is a relatively weakly bound state, $D_e \approx 16$ kcal/mol, located some 19,000 cm^{-1} above the X state at $r_e = 1.95$ Å (Table 5). It arises by removing a p_π electron from the $a\,^3\Pi$ state of ClF. The bonding interaction between Cl$^+$(^{3}P) + F(^{2}P) is captured by the following vbL icon, analogous to that of the $a\,^3\Pi$ state (vide supra).

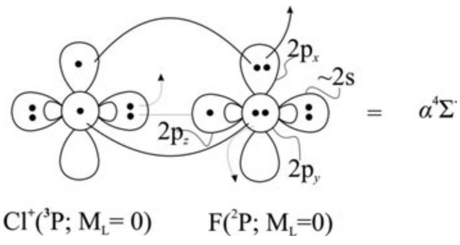

The leading MRCI configurations are

$$\left|a^4\Sigma^-\right\rangle \approx \left|1\sigma^2 2\sigma^2 3\sigma^2 4\sigma^1 [(0.82)1\pi_x^2 2\pi_x^1 - (0.24)1\pi_x^1 2\pi_x^2] 1\pi_y^2 2\pi_y^1\right\rangle - 0.24\left|1\sigma^2 2\sigma^2 3\sigma^2 4\sigma^1 1\pi_x^2 2\pi_x^1 1\pi_y^1 2\pi_y^2\right\rangle$$

very similar to the leading configurations of the $a\,^3\Pi$ (ClF) state. A total charge of 0.15 e$^-$ is transferred from F to Cl$^+$ according to the Mulliken analysis. The contrast of the numerical parameters between $a\,^4\Sigma^-$ and $a\,^3\Pi$ (ClF) shows clearly the analogy between these two states. Indeed, at the MRCI + Q/A6ζ level, we have ($a\,^3\Pi$ results in parenthesis): $r_e = 1.9475$ (2.0144) Å, $D_e = 16.10$ (8.70) kcal/mol, $T_e = 18{,}649$ (18,996) cm^{-1}; see Table 5. The almost doubling of D_e of the $a\,^4\Sigma^-$ state as compared to the $a\,^3\Pi$, is due to an extra 3e$^-$ − 2c p_π "bond" of the former; see the corresponding vbL diagrams. Core and relativistic effects are practically negligible in the $a\,^4\Sigma^-$ state. For instance, the $X\,^2\Pi$–$a\,^4\Sigma^-$ gap (T_e) at the MRCI + Q/A5ζ level increases by 173 and decreases by 175 cm^{-1} due to core and relativistic effects, respectively. Finally, it is interesting to observe that the MRCI + Q/A5ζ r_e and D_e values reported in Ref. [33] are by 0.025 Å larger and 2.5 kcal/mol smaller than the present ones.

Table 6 Total energies E (E_h), bond distances r_e (Å), dissociation energies D_e and D_0 (kcal/mol), harmonic frequencies ω_e (cm^{-1}) and anharmonicities $\omega_e x_e$ (cm^{-1}), rotational vibrational coupling constant α_e (cm^{-1}), and adiabatic electron affinity EA$_{ad}$ (eV) of the $X\,^2\Sigma^+$ state of the ^{35}Cl^{19}F$^-$ anion

Method	$-E$	r_e	D_e^a	$D_0^{a,b}$	ω_e	$\omega_e x_e$	$\alpha_e \times 10^3$	EA$_{ad}$
MRCI + Q/A5ζ	559.53667	2.159	30.32	29.78	375.0	2.40	2.69	2.17
MRCI + Q/A6ζ	559.54233	2.151	30.33	29.80	373.0	3.50	4.06	2.16
RCCSD(T)/A5ζ	559.54378	2.1643	30.14	29.62	364.0	2.62	3.00	2.26
RCCSDT/A5ζ	559.54389	2.1640	29.47					2.23
RCCSD(T)/A6ζ	559.54977	2.1644	29.82	29.30	363.4	2.51	3.08	2.26
CCSD(T)/A5ζ[c]		2.1531			378			2.25
Expt.[d]								2.86 ± 0.2

[a] With respect to Cl$^-$(^{1}S) + F(^{2}P)

[b] $D_0 = D_e - \omega_e/2 + \omega_e x_e/4$

[c] Ref. [32]

[d] Ref. [44]

3.2.3 $2^2\Pi$, $3^2\Pi$

These two $^2\Pi$ states correlate adiabatically with the first ($2^2\Pi$) and with the second ($3^2\Pi$) energy channels. The repulsive $2^2\Pi$ state, however, suffers a severe avoided crossing with the incoming $3^2\Pi$ (attractive) state around 4 bohr; see inset of Fig. 2. It seems that the only experimental finding relevant to this energy region is an ionization–excitation energy in very good agreement with the MRCI + Q/A5ζ calculated value, 16.39 ± 0.01 [38] versus 16.15 eV. At this level of theory T_e ($2\ ^2\Pi \leftarrow X\ ^2\Pi$) = 28,587 cm^{-1}, D_e (D_0) = 20.6 (20.0) kcal/mol with respect to the diabatic fragments $Cl^+(^1D) + F(^2P)$, and r_e = 2.00 Å. In Table 5, and with a grain of salt, results are also given for the $3^2\Pi$ (pseudo) state.

3.2.4 Higher states of ClF^+

We discussed three bound states of ClF^+, $X\ ^2\Pi$, $a\ ^4\Sigma^-$, and $2\ ^2\Pi$, all correlating adiabatically with the first channel $Cl^+(^3P) + F(^2P)$. The rest of the states, nine from the first and eight from the second channels, are weakly bound or of repulsive nature never characterized before either experimentally or theoretically; see Fig. 2. The nine states split naturally in two sheafs of five (lower) and four (higher) states each. The symmetries of the first five states are (in parenthesis equilibrium minima r_e in Å and attractive interaction energies $-\Delta E$ in kcal/mol) $1^4\Delta$ (2.48, 4.2), $1^4\Sigma^+$ (2.49, 4.6), $1^2\Sigma^-$ (2.65, 3.50), $1^2\Delta$ (2.61, 3.3), and $1^2\Sigma^+$ (2.68, 2.9) at a mean separation energy of $\bar{T}_e$ = 23,609 cm^{-1}. The next four states of symmetries $1^4\Pi$, $2^2\Sigma^-$, $2^4\Sigma^-$, and $2^4\Pi$ are of repulsive character but the $1^4\Pi$, where r_e = 3.27 Å and ΔE = −1.19 kcal/mol at T_e = 24,568 cm^{-1}; see Fig. 2.

We now turn to the eight doublets which emerge from the second channel. The first three at a mean $\bar{T}_e$ = 34,067 cm^{-1} can be considered as slightly bound, namely $2^2\Delta$ (r_e = 2.35 Å, D_e = 6.9 kcal/mol), $3^2\Sigma^-$ (2.41, 6.8), and $2^2\Sigma^+$(2.47, 5.3). The first of the remaining five states, $4^2\Pi$, shows a well depth of ΔE = −1.3 kcal/mol at r_e = 3.25 Å, while states of symmetries $1^2\Phi$, $3^2\Sigma^+$, $5^2\Pi$, and $3^2\Delta$ are repulsive. The last two PECs calculated at the MRCI + Q/A5ζ level of theory originate from the third channel, $Cl^+(^1S) + F(^2P)$, of $6^2\Pi$ and $4^2\Sigma^+$ symmetries; their PECs are not shown in Fig. 2. The $4^2\Sigma^+$ state is purely repulsive, whereas the $6^2\Pi$ interacts attractively at r_e = 2.71 Å with ΔE = −3.8 kcal/mol and T_e = 50,995 cm^{-1}.

3.3 ClF^-

Molecular anions are not easily tamed species either theoretically or experimentally. For an exhaustive review referring to atomic and molecular electron affinities and the difficulties of obtaining reliable results, see Ref. [45] and references cited therein. As was already discussed in Sect. 1, the only structural parameter that has been measured on ClF^- is its ionization energy, or the adiabatic electron affinity of ClF, the most recent value being EA_{ad} = 2.86 ± 0.2 eV [44], a strongly disputed number (see the Sect. 1). For the best ab initio work so far on ClF^-, we refer to Horný et al. [32]; see also Sect. 1 and Table 6.

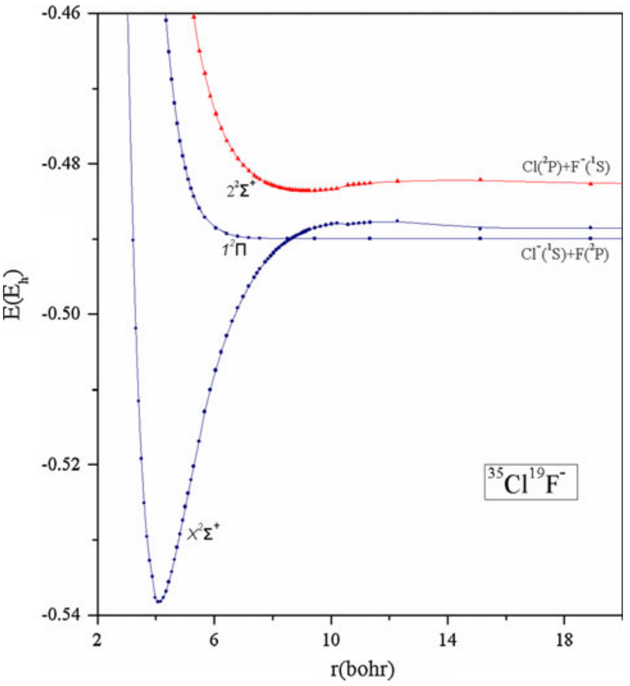

Fig. 3 Relative MRCI + Q/A5ζ PECs of two (*first channel*) and one (*second channel*) states of ClF^-

The EAs of $Cl(^2P)$ and $F(^2P)$ are 3.612724 ± 0.000027 [80] and 3.4011895 ± 0.0000025 eV [81], respectively. Theoretical EAs at the MRCI + Q (RCCSD(T))/A6ζ level of theory are 3.574 (3.659) and 3.450 (3.414) eV, respectively. It should be said at this place that bound excited states (not resonances) of atomic anions are not common. In particular, it is rather certain that there are no excited states of $Cl^-(^1S)$ and $F^-(^1S)$ [82, 83], despite the high EAs of these atoms, as a matter of fact the highest of all elements [84]. According to the discussion above, one expects four molecular $^{2S+1}\Lambda$ states of $^2\Pi$ and $^2\Sigma^+$ symmetry, related to the channels $Cl^-(^1S) + F(^2P)$, and $Cl(^2P) + F^-(^1S)$, the experimental energy difference between the two adiabatic end products being ΔEA_{ad} = 0.212 eV.

Table 6 lists spectroscopic parameters for the $X\ ^2\Sigma^+$ state of $^{35}ClF^-$, while Fig. 3 displays state-specific MRCI + Q/A5ζ PECs of the $X\ ^2\Sigma^+$, $1^2\Pi$ and $2^2\Sigma^+$ states. The fourth $2^2\Pi$ state, repulsive in character, is not shown because of severe technical problems.

3.3.1 $X\ ^2\Sigma^+$

The ground state of ClF^- correlates adiabatically with $\mathrm{Cl}^-(^1\mathrm{S}) + \mathrm{F}(^2\mathrm{P})$. The vbL diagram, MRCI leading equilibrium configuration, and Mulliken population distributions around equilibrium (r_e) and at infinity (r_∞) presented below allow for a better understanding of the considerable binding energy of the $X\ ^2\Sigma^+$ state, $D_\mathrm{e} \sim 30$ kcal/mol.

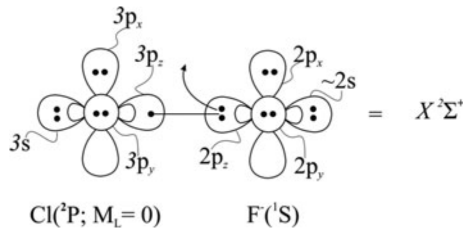

$$\left|X^2\Sigma^+\right\rangle \approx 0.93\left|1\sigma^2 2\sigma^2 3\sigma^2 4\sigma^1 1\pi_x^2 1\pi_y^2 2\pi_x^2 2\pi_y^2\right\rangle$$

$$\mathrm{r_e}: 3s^{1.98}3p_z^{1.37}3p_x^{1.97}3p_y^{1.97}/_{\mathrm{Cl}}2s^{1.98}2p_z^{1.59}2p_x^{1.98}2p_y^{1.98}/_{\mathrm{F}}$$
$$\mathrm{r}_\infty: 3s^{1.99}3p_z^{1.95}3p_x^{1.97}3p_y^{1.97}/_{\mathrm{Cl}}2s^{1.99}2p_z^{1.02}2p_x^{1.99}2p_y^{1.99}/_{\mathrm{F}}$$

Overall about 0.6 e^- seems to be transferred from Cl^- to F around the equilibrium distance at the MRCI/A5ζ or A6ζ level. However, the morphology of the PECs suggests that due to an interaction at ∼9.5 bohr between the $X\ ^2\Sigma^+$ and $2^2\Sigma^+$ states, the latter correlating with $\mathrm{F}^-(^1\mathrm{S}) + \mathrm{Cl}(^2\mathrm{P})$, ∼0.4 e^- are transferred from F^- to Cl around equilibrium.

According to Table 6, the RCCSD(T)/A6ζ (RCCSDT/A5ζ), $\mathrm{EA_{ad}} = 2.26$ (2.23) eV at $r_\mathrm{e} = 2.164$ Å, in practical agreement with the $\mathrm{EA_{ad}}$ of Horný et al. [32] who at the CCSD(T)/A5ζ level predict $\mathrm{EA_{ad}} = 2.25$ eV; MRCI + Q/A5ζ or A6ζ $\mathrm{EA_{ad}}$ is by 0.1 eV less. We believe that this settles definitely the question of the $\mathrm{EA_{ad}}$ of $\mathrm{ClF}(X\ ^1\Sigma^+)$. Using this value and the experimental binding energy of ClF along with the experimental EA of Cl, the "experimental" dissociation energy of ClF^- is $D_0(\mathrm{ClF}^-) = D_0(\mathrm{ClF})–[\mathrm{EA(Cl)} - \mathrm{EA_{ad}(ClF)}] = 60.35$ kcal/mol − (3.6127 − 2.26) eV = 29.16 kcal/mol, completely consistent with the CC results and in excellent agreement with the MRCI + Q results of Table 6. Thus, the recommended D_0 value of the $X\ ^2\Sigma^+$ state of ClF^- is 29.5 kcal/mol. It should be added at this point that core and relativistic effects at the RCCSD(T)/A5ζ level reduce the bond distance by 0.002 and 0.001 Å, respectively. Therefore, our "best" bond distance is $r_\mathrm{e}{}^* = 2.161$ Å.

3.3.2 $1^2\Pi$

This state correlates with $\mathrm{Cl}^-(^1\mathrm{S}) + \mathrm{F}(^2\mathrm{P};\ \mathrm{M} = \pm 1)$. The congestion of four electrons in the σ-frame is the cause of a pure repulsive $1^2\Pi$ state the MRCI + Q/A5ζ PEC of which is shown in Fig. 3.

3.3.3 $2^2\Sigma^+$

The MRCI + Q/A5ζ PEC of $2^2\Sigma^+$ state correlates with $\mathrm{F}^-(^1\mathrm{S}) + \mathrm{Cl}(^2\mathrm{P};\ M = 0)$ presenting a well depth of 0.82 kcal/mol at about 9.2 bohr; see Fig. 3.

4 Epitome and remarks

We believe that the present work is a systematic theoretical study of the interhalogen diatomic ClF and its ions $\mathrm{ClF}^\pm$ within the $\Lambda - S$ ansatz. Despite the chemical simplicity of the X_2 and XX′ (X, X′ = F, Cl, Br, I) molecules, the determination of reliable properties either experimentally or theoretically is a daunting task. Even for the lightest interhalogen species (ClF), the large number of valence electrons (14), the relative weak bonding, and the intervening spin–orbit effects create a challenging computational *milieu*. Although this investigation leaves much to be done for the $\mathrm{ClF}^{0,\pm}$ systems, particularly for the higher states, some of our results are very accurate, some have been calculated for the first time, and in general a wealth of new information is enclosed in this communication useful to workers with some interest in these systems.

Through the use of augmented quintuple and sextuple correlation consistent basis sets, thus in essence removing the error related to the one-electron basis set at least for the lowest states, and multireference CI (MRCI) and single-reference CC (RCCSD(T), RCCSDT) calculations, we have examined a significant number of states of ClF and $\mathrm{ClF}^\pm$. In particular, we have constructed full potential $^{2S+1}\Lambda$ energy curves for all states of ClF emanating from the first channel (12), all states of ClF^+ emanating from the first three channels of $\mathrm{Cl}^+ + \mathrm{F}$ (23), and three states out of four correlating with $\mathrm{Cl}^-(^1\mathrm{S}) + \mathrm{F}(^2\mathrm{P})$ or $\mathrm{Cl}(^2\mathrm{P}) + \mathrm{F}^-(^1\mathrm{S})$ for the ClF^- anion. A number of states have been corrected for core ($2s^22p^6/_{\mathrm{Cl}}$), scalar relativistic, and SO effects. Size non-extensivity errors were taken into account through the +Q Davidson correction. The most salient features of the present work are summarized below.

4.1 ClF

The ground state of ClF is of $^1\Sigma^+$ symmetry; MRCI + Q calculated (experimental) values are $D_0^0 = 60.35$ (60.35) kcal/mol, $r_\mathrm{e} = 1.6284$ (1.628341(4)) Å, $\omega_\mathrm{e} = 786.1$ (783.353) cm^{-1}, $\mu_\mathrm{e} = 0.878$ (0.8881) Debye with a charge polarity $^{+q}\mathrm{Cl} - \mathrm{F}^{-q}$, q = 0.25. Excellent agreement is obtained at the CC level as well. The single σ bond can be adequately described by one configuration function; indeed, $|C_0|^2 \approx 0.9$.

$a\ ^3\Pi$ is the first and only within the $\Lambda - S$ coupling scheme bound state related to ground-state fragments. Its binding energy is about an order of magnitude less than that of the $X\ ^1\Sigma^+$ state. A weak Paschen–Back effect is the cause of the $\Omega = 2, 1, 0^+$ (0^-) components of the $a\ ^3\Pi$ state, named A′, A, and B, respectively, for historical reasons; no name has been adopted for the 0^- state. Notice that the splitting between the $0^+ - 0^-$ components is very small [3] and in the present work $^3\Pi_{0^\pm} = {}^3\Pi_0$. Our "best" MRCI + Q calculated (experimental results referring to $^3\Pi_{0^+}$) values are $D_e^0 = 8.75$ (8.802) kcal/mol, $r_e = 2.0145$ (2.0221) Å, $\omega_e = 366.6$ (362.6) cm^{-1}, $\mu_e = 1.583$ D (no experiment), and $T_e = 18{,}864$ (18,825.3) cm^{-1}. This is a multireference state; therefore, CC calculations are not recommended for its computation. Within the $\Lambda - S$ treatment, there are nine strongly repulsive PECs and a van der Waals $1^1\Pi$ state, the latter with an interaction energy of less than 0.5 kcal/mol and r(vdW) = 3.31 Å at the MRCI + Q level.

4.2 ClF^+

The ground state of ClF^+ is of $^2\Pi$ symmetry. We have detected three $\Lambda - S$ bound states $X\ ^2\Pi$, $a\ ^4\Sigma^-$, and $2^2\Pi$, whereas for the latter two the experimental data are practically none.

For the $X\ ^2\Pi$ state, our MRCI + Q/A6ζ calculated (experimental) values are $D_0^0 = 67.40$ (67.43) kcal/mol, $r_e = 1.5357$ (1.53) Å, $\omega_e = 913.7$ (912) cm^{-1}, and IE = 12.61 (12.66) eV. CC results are in very good agreement as well. The dissociation energy of the $X\ ^2\Pi$ state is by $\Delta D = 7.1$ kcal/mol larger than that of the $X\ ^1\Sigma^+$ of ClF, whereas Δr_e $(X\ ^2\Pi - X\ ^1\Sigma^+) = -0.093$ Å.

Our MRCI + Q/A6ζ results for the $a\ ^4\Sigma^-$ state, a rather "dark" state for the experimentalists, are $D_0 = 15.54$ kcal/mol, $r_e = 1.9475$ Å, $\omega_e = 398.5$ cm^{-1}, and $T_e = 18{,}649$ cm^{-1}. Notice also that in line with the $a\ ^3\Pi$ state of ClF, $\Delta D = 6.74$ kcal/mol and $\Delta r_e = -0.04$ Å.

For the $2^2\Pi$ state, our MRCI + Q/A5ζ calculations predict $D_0 = 20.0$ kcal/mol, $r_e = 2.00$ Å, $\omega_e = 410$ cm^{-1}, and $T_e = 28{,}587$ cm^{-1}. It is interesting that there is a remarkable agreement with an experimental ionization–excitation energy, 16.39 ± 0.01 eV versus 16.15 eV, proving that the "tentative" assignment of the experimentalists [38] is correct.

4.3 ClF^-

The ground state of ClF^- is of $^2\Sigma^+$ symmetry. The only experimental datum is the (adiabatic) electron affinity EA_{ad} [ClF $(X\ ^1\Sigma^+) + e^- \rightarrow ClF^-(X\ ^2\Sigma^+)$] = 2.86 ± 0.2 eV, proved to be wrong by ~+0.6 eV. Our RCCSDT/A5ζ [RCCSD(T)/A6ζ] (MRCI + Q/A6ζ) = 2.23 [2.26] (2.16) eV value, in agreement with previous CC calculations. Clearly, our calculations converge to an EA_{ad} of 2.25 ± 0.01 eV. The MRCI + Q/A6ζ predictions for this state are $D_0^0 = 29.80$ kcal/mol, $r_e = 2.151$ Å, and $\omega_e = 373.0$ cm^{-1}. A charge of 0.4 e^- is transferred from the in situ F^- to Cl around the equilibrium.

The four homonuclear and six heteronuclear dihalogens, XX′ (X, X′ = F, Cl, Br, I) are of emblematic importance for chemistry. We tried to present here a useful theoretical account of the behavior and properties of $ClF^{0,\pm}$, but obviously the subject is far from being closed and further investigation experimental and theoretical as well is clearly needed. We hope that our future work will move toward this direction, particularly toward the excited manifold of these fascinating species.

Acknowledgments One of us (A.V.) expresses his gratitude to Dr. C. N. Sakellaris for helpful discussions.

References

1. Dicciani NK, Burrows C, Greenspan A, Stang PJ (2003) Chem Eng News (number 36), 81, pp. 48(F), *62*(Cl), 96(Br), and 130(I)
2. Greenwood NN, Earnshaw A (1998) Chemistry of the elements, 2nd edn. Butterworth–Heinemann, Oxford, pp 824–825
3. Huber KP, Herzberg G (1979) Molecular spectra and molecular structure. IV constants of diatomic molecules, Van Nostrand Reinhold Co, NY
4. Wahrhaftig AL (1942) J Chem Phys 10:248
5. Gilbert DA, Roberts A, Griswold PA (1949) Phys Rev 76:1723
6. Stricker W, Krauss L (1968) Z Naturforsch 23a:1116
7. Dibeler VH, Walker JA, McCulloh KE (1970) J Chem Phys 53:4414
8. Davis RE, Muenter JS (1972) J Chem Phys 57:2836
9. Nordine PC (1974) J Chem Phys 61:224
10. Combe RD, Pilipovich D, Horne RK (1978) J Phys Chem 82:2484
11. Willis RE Jr, Clark WW III (1980) J Chem Phys 72:4946
12. McDermid IS (1981) J Chem Soc Faraday Trans 2(77):519
13. McDermid IS, Laudenslager JB (1981) Chem Phys Lett 79:370
14. Alekseev VA, Setser DW (1997) J Chem Phys 107:4771
15. Jenkins FA (1953) J Opt Soc Am 43:425
16. Alekseev VA, Setser DW, Tellinghuisen J (1999) J Mol Spectrosc 61:194
17. Alekseev VA, Setser DW, Tellinghuisen J (1999) J Mol Spectrosc 195:162
18. Schmitz H, Schumacher HJ (1947) Z Naturforsch 2a:359
19. Schumacher HJ, Schmitz H, Brodersen PH (1950) Anales Asoc Quim Argent 38:98
20. Straub PA, McLean AD (1974) Theor Chim Acta 32:227
21. Ewig CS, Sur A, Banna MS (1981) J Chem Phys 75:5002
22. Scharf P, Ahlrichs R (1985) Chem Phys 100:237
23. Darvesh KV, Boyd RJ, Peyerimhoff SD (1988) Chem Phys 121:361
24. Peterson KA, Woods RC (1990) J Chem Phys 92:7412
25. Perera SA, Bartlett RJ (1993) Chem Phys Lett 216:606 and references therein
26. deJong WA, Styszynski J, Visscher L, Nieuwpoort WC (1998) J Chem Phys 108:5177 and references therein

27. Alekseyev AB, Liebermann HP, Buenker RJ, Koch KB (2000) J Chem Phys 112:2274 and references therein
28. Buenker RJ, Peyerimhoff SD (1974) Theor Chim Acta 35:33
29. Buenker RJ, Peyerimhoff SD (1975) Theor Chim Acta 39:217
30. Buenker RJ, Peyerimhoff SD, Butsher W (1978) Mol Phys 35:771
31. Ricca A (2000) Chem Phys Lett 323:498
32. Horný L, Sattelmeyer KW, Schaefer HF III (2003) J Chem Phys 119:11615
33. Chen L, Woon DE, Dunning TH Jr (2009) J Phys Chem A 113:12645
34. Chen L, Woon DE, Dunning Jr. TH (2013) J Phys Chem A 117:4251 and references therein.
35. Kalemos A, Mavridis A (2009) J Phys Chem A 113:13972
36. Kalemos A, Mavridis A (2011) J Phys Chem A 115:2378 and references therein
37. Irsa AP, Friedman L (1958) J Inorg Nucl Chem 6:77
38. Anderson CP, Mamantov G, Bull WE, Grimm FA, Carver JC, Carlson TA (1971) Chem Phys Lett 12:137
39. De Kock RL, Higginson BR, Lloyd DR, Breeze A, Cruickshank DWJ, Armstrong DR (1972) Mol Phys 24:1059
40. Radziemski LJ, Kaufmann V (1969) J Opt Soc Am 59:424
41. Harland P, Thynne JCJ (1969) J Phys Chem 73:4031
42. Dispert H, Lacmann K (1978) Int J Mass Spectrom Ion Phys 28:49
43. Illenberger E, Scheunemann HU, Baumgärtel H (1979) Chem Phys 37:21
44. Dudlin AV, Gorokhov LN, Baluev AV (1979) Izv Akad Nauk SSR Ser Khi 11:2408
45. Rienstra-Kiracofe JC, Tschumper GS, Schaefer HF III (2002) Chem Rev 102:231
46. Curtiss LA, Raghavachari K, Redfern PC, Rassolov V, Pople JA (1998) J Chem Phys 109:7764
47. Curtiss LA, Redfern PC, Raghavachari K, Pople JA (2001) J Chem Phys 114:108
48. Law CK, Chien SH, Li WK, Cheung YS (2002) J Phys Chem A 106:11271
49. Dunning TH Jr (1989) J Chem Phys 90:1007
50. Kendall RA, Dunning TH Jr, Harrison RJ (1992) J Chem Phys 96:6796
51. Dunning TH Jr, Peterson KA, Wilson AK (2001) J Chem Phys 114:9244
52. Wilson AK, van Mourik T, Dunning TH Jr (1997) J Mol Struct (THEOCHEM) 388:399
53. Woon DH, Dunning TH Jr (1993) J Chem Phys 98:1358
54. Raghavachari K, Trucks GW, Pople JA, Head-Gordon M (1989) Chem Phys Lett 157:479
55. Watts JD, Gauss J, Bartlett RJ (1993) J Chem Phys 98:8718
56. Knowles PJ, Hampel C, Werner HJ (1993) J Chem Phys 99:5219
57. Knowles PJ, Hampel C, Werner HJ (2000) J Chem Phys 112:3106
58. Werner HJ, Knowles PJ (1988) J Chem Phys 89:5803
59. Knowles PJ, Werner HJ (1988) Chem Phys Lett 145:514
60. Douglas M, Kroll NM (1974) Ann Phys 82:89
61. Hess BA (1985) Phys Rev A 32:756
62. Jansen HB, Ross P (1969) Chem Phys Lett 3:140
63. Boys SF, Bernardi F (1970) Mol Phys 19:553
64. Dunham JL (1932) Phys Rev 41:721
65. Herzberg G (1950) Molecular spectra and molecular structure 1. Spectra of diatomic molecules, 2nd edn. D. van Nostrand Co, Inc., Canada
66. Langhoff RS, Davidson ER (1974) Int J Quantum Chem 8:61
67. Davidson ER, Silver DW (1977) Chem Phys Lett 52:403
68. Sakellaris CN, Mavridis A (2012) J Chem Phys 137:034309
69. CFOUR, a quantum chemical program package written by Stanton JF, Gauss J, Harding ME, Szalay PG with contributions from Auer AA, Bartlett RJ, Benedikt U, Berger C, Bernholdt DE, Bomble YJ, Cheng L, Christiansen O, Heckert M, Heun O, Huber C, Jagau T-C, Jonsson D, Jusélius J, Klein K, Lauderdale WJ, Matthews DA, Metzroth T, Mück LA, O'Neill DP, Price DR, Prochnow E, Puzzarini C, Ruud K, Schiffmann F, Schwalbach W, Stopkowicz S, Tajti A, Vázquez J, Wang F, Watts JD and the integral packages *MOLECULE* (J. Almlöf and P.R. Taylor), *PROPS* (P.R. Taylor), *ABACUS* (Helgaker T, Jensen HJ, Jørgensen P, Olsen J), and ECP routines by Mitin AV, van Wüllen C. For the current version, see http://www.cfour.de
70. MOLPRO is a package of ab initio programs written by Werner H-J, Knowles PJ, Knizia G, Manby FR, Schütz M, Celani P, Korona T, Lindh R, Mitrushenkov A, Rauhut G, Shamasundar KR, Adler TB, Amos RD, Bernhardsson A, Berning A, Cooper DL, Deegan MJO, Dobbyn AJ, Eckert F, Goll E, Hampel C, Hesselmann A, Hetzer G, Hrenar T, Jansen G, Köppl C, Liu Y, Lloyd AW, Mata RA, May AJ, McNicholas SJ, Meyer W, Mura ME, Nicklaß A, O'Neill DP, Palmieri P, Peng D, Pflüger K, Pitzer R, Reiher M, Shiozaki T, Stoll H, Stone AJ, Tarroni R, Thorsteinsson T, Wang M
71. Kramida A, Ralchenko Yu, Reader J, and NIST ASD Team (2012). NIST atomic spectra database (ver. 5.0), [Online]. Available: http://physics.nist.gov/asd [5 June 2013]. National Institute of Standards and Technology, Gaithersburg, MD
72. Tzeli D, Mavridis A (2003) J Chem Phys 118:4984
73. Ewing JJ, Tigelaar HL, Flygare WH (1972) J Chem Phys 56:1957
74. McGurk J, Noris CL, Tigelaar HL, Flygare WH (1973) J Chem Phys 58:3118
75. Green J (1974) Adv Chem Phys 25:179
76. Janda KC, Klemperer W, Novick SE (1976) J Chem Phys 64:2698
77. Fabricant B, Muenter JS (1977) J Chem Phys 66:5274
78. Magoulas I, Kalemos A, Mavridis A (2013) J Chem Phys 138:104312
79. Edlén B (1969) Sol Phys 9:439
80. Berzinsh U, Gustafson M, Hanstorp D, Klinkmüller A, Ljungblad U, Martensson-Pendrill AM (1995) Phys Rev A 51:231
81. Blondel C, Delsart C, Goldfarb F (2001) J Phys B 34:L281
82. Andersen T (1991) Phys Scr 43:23
83. Hogrere H (1998) Phys Scr 58:25
84. Emsley J (1991) The elements, 2nd edn. Clarendon Press, Oxford